

HIGH-SENSITIVITY *IRAS*<sup>1</sup> OBSERVATIONS OF THE CHAMAELEON I DARK CLOUDB. BAUD, E. YOUNG, C. A. BEICHMAN, D. A. BEINTEMA, J. P. EMERSON, H. J. HABING, S. HARRIS,  
R. E. JENNINGS, P. L. MARSDEN, AND P. R. WESSELIUS*Received 1983 September 14; accepted 1983 November 21*

## ABSTRACT

Very sensitive *IRAS* observations of a region of  $0.8 \text{ deg}^2$  in the Chamaeleon I cloud have revealed 70 compact sources. Hot sources are field stars; warm sources are associated with pre-main-sequence (PMS) stars in the cloud center; others may be in an even earlier phase of gravitational collapse. Cool sources, detected only at the long wavelengths, surround the main cloud and appear to be associated with small globules. Only a small fraction ( $< 20\%$ ) of the total luminosity of the known PMS objects is emitted in the *IRAS* bands. This has important implications for the classification of the newly discovered embedded objects.

*Subject headings:* infrared: sources — nebulae: general — stars: formation — stars: pre-main-sequence

## I. INTRODUCTION

In this *Letter* the first results are described from special pointed observations with the *IRAS* satellite of  $0.8 \text{ deg}^2$  in the Chamaeleon I dark cloud. Because the cloud is nearby (215 pc; Hyland, Jones, and Mitchell 1982, hereafter HJM) and at high galactic ( $-15^\circ$ ) and ecliptic ( $-65^\circ$ ) latitudes, objects of very low infrared luminosity can be studied without confusion from asteroids or background galactic emission. Like the Taurus cloud, Cha I contains many low-mass pre-main-sequence (PMS) objects such as  $H\alpha$  emission-line stars, Herbig-Haro objects, and embedded near-infrared objects (e.g., HJM; Schwartz 1977). Cha I is, however, smaller than Taurus and can be studied more completely at much higher sensitivity than the regular survey provides.

## II. OBSERVATIONS AND DATA PROCESSING

The *IRAS* instrument is described in detail by Neugebauer *et al.* (1984, hereafter Paper I). Nine pointed observations were made during which the survey instrument scanned a rectangular field of  $1.6^\circ \times 0.5^\circ$ . The maps at each of the four wavelengths were added and averaged. Each individual map was compared with the final, average map to search for spurious sources such as detector spikes or asteroids. No such sources were found. The four final maps were searched for compact ( $< 1'$ ) sources by computer. For confused sources, positions and in-band fluxes were determined by hand from the maps. Occasionally, strong confusion at 60 and  $100 \mu\text{m}$  made a flux determination impossible. Sources from different bands within  $1'$  from each other were then merged. The in-band fluxes of the 70 band-merged sources with a signal-to-noise ratio greater than 4 were color-corrected (Paper I) and converted to  $\text{Jy}$  ( $10^{-26} \text{ W m}^{-2} \text{ Hz}^{-1}$ ). They are listed in Table 1. The  $3\sigma$  noise levels in the final maps are: 0.02, 0.02, 0.03, and  $0.28 \text{ Jy}$  at 12, 25, 60, and  $100 \mu\text{m}$ , respectively, about

a factor of 10 lower than in the all-sky survey. We adopt an uncertainty in the absolute photometric calibration of  $\pm 30\%$  (Paper I).

## III. RESULTS

a) *Distribution and Nature of the Sources*

The photograph in Figure 1 (Plate L1) shows the distribution of sources in the deep-sky field on the Chamaeleon cloud. The field covers from west to east three distinct regions: (1) a region of low, but clearly visible, extinction with several small pockets of high extinction interspersed; (2) the cloud center, which is completely opaque and contains two reflection nebulae; and (3) a region of very little or almost no extinction, just east of a steep gradient in the extinction that defines the cloud boundary.

The remarkably uniform source distribution is probably due to a mixture of different classes of objects. We have therefore divided the majority of the sample in four subsamples of increasingly redder spectra. Their spatial distributions are shown in Figure 2.

Hot sources have  $F_\nu(12 \mu\text{m})/F_\nu(25 \mu\text{m}) > 3-4$ , typical for normal stars with a blackbody temperature of 1000–3000 K. The distribution in Figure 2 is very uniform across the field, as expected from unrelated field stars. Inspection of the photograph confirms in most cases the presence of one or two relatively bright stars within the circle.

Warm sources have  $F_\nu(60 \mu\text{m}) > F_\nu(25 \mu\text{m})$ . Their infrared colors suggest the presence of a central object surrounded by a circumstellar dust shell with a temperature range of 70–200 K for grains with a  $\nu^1$  emissivity. Unlike the hot sources, most warm objects (13 out of 17) lie well within the cloud boundaries. Inspection of the plate shows that, in many cases, weak nebulosities are seen near the infrared position. One warm source (14) is an edge-on galaxy. The concentration of warm sources and their relatively low 60–25  $\mu\text{m}$  flux density ratio of about 4, compared to a value of 10 for field galaxies found in the all-sky survey (Soifer *et al.* 1984), suggests that

<sup>1</sup>The *Infrared Astronomical Satellite* was developed and is operated by the Netherlands Agency for Aerospace Programs (NIVR), the US National Aeronautics and Space Administration (NASA), and the UK Science and Engineering Research Council (SERC).

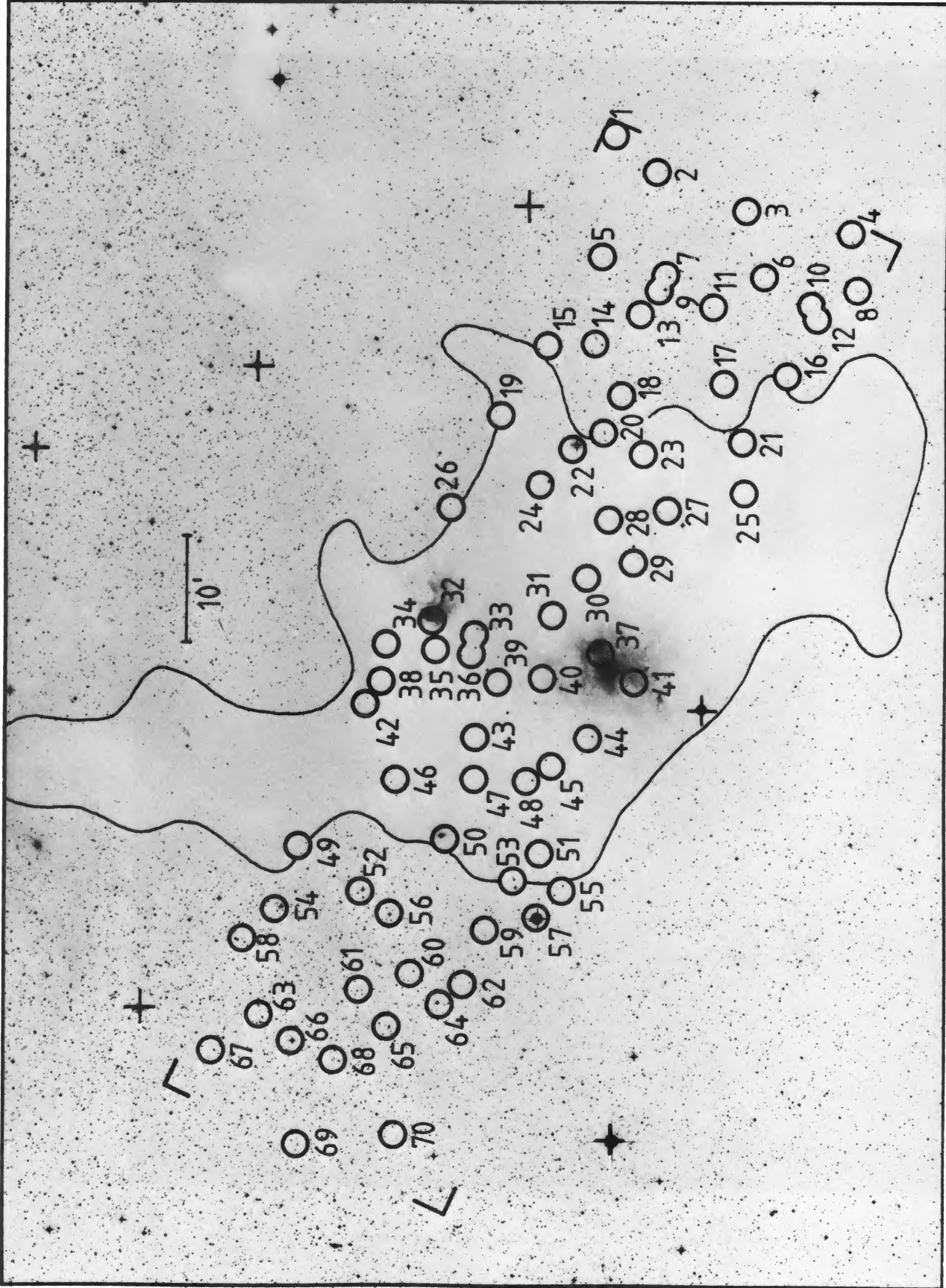


FIG. 1.—Distribution of IRAS sources on a European Southern Observatory/Science Research Council film of the Chamaeleon dark cloud complex. The circles have a diameter of 3'. Source number from Table 1 appears below or on the side of the circle. The corners of the deep-sky field are indicated. Continuous line represents the cloud boundary. BAUD *et al.* (see page L53)

TABLE 1  
CHAMAELEON IRAS SOURCE LIST

No. (1)	12 $\mu$ m (Jy) (2)	25 $\mu$ m (Jy) (3)	60 $\mu$ m (Jy) (4)	100 $\mu$ m (Jy) (5)	No. (1)	12 $\mu$ m (Jy) (2)	25 $\mu$ m (Jy) (3)	60 $\mu$ m (Jy) (4)	100 $\mu$ m (Jy) (5)
1.....	...	0.03	...	...	36.....	0.15	...	...	...
2.....	...	...	0.06	...	37.....	1.29	C	...	...
3.....	...	...	0.07	...	38.....	0.23	0.28	0.34	...
4.....	...	...	0.17	...	39.....	0.04	...	...	...
5.....	...	...	...	0.43	40.....	9	20	> 30	C
6.....	0.22	0.09	...	...	41 <sup>a</sup> .....	13	80	300	C
7.....	0.20	0.06	0.05	...	42.....	0.03	0.14	0.48	...
8.....	0.06	...	...	...	43.....	0.07	0.14	0.28	C
9.....	0.05	...	...	...	44.....	0.68	0.52	0.07	...
10.....	...	...	0.05	...	45.....	0.32	0.40	0.33	...
11.....	...	...	...	0.44	46.....	0.31	0.77	1.0	...
12.....	...	...	...	0.51	47.....	0.07	0.10	0.23	C
13.....	...	...	...	1.00	48.....	0.17	...	...	...
14.....	0.04	0.05	0.48	...	49.....	...	...	0.06	...
15.....	...	...	...	1.70	50.....	0.04	0.13	1.3	7.9
16.....	...	...	0.06	...	51.....	...	...	0.05	...
17.....	...	...	0.14	...	52.....	0.11	0.04	...	...
18.....	...	...	0.11	...	53.....	0.59	0.02	...	...
19.....	...	...	0.04	...	54.....	...	0.03	...	...
20.....	0.03	...	...	...	55.....	...	0.02	C	C
21.....	...	...	0.05	...	56.....	...	...	0.11	...
22.....	0.03	...	...	...	57.....	0.12	0.03	...	...
23.....	...	0.15	0.22	2.34	58.....	0.10	0.02	...	...
24.....	0.03	0.84	3.78	...	59.....	...	...	0.12	C
25.....	...	...	0.04	...	60.....	...	0.04	C	...
26.....	...	...	0.11	...	61.....	...	0.07	0.47	C
27.....	...	...	0.04	C	62.....	0.03	...	...	...
28.....	0.09	0.03	...	C	63.....	0.10	0.23	0.89	...
29.....	...	0.08	0.30	...	64.....	0.04	...	...	...
30.....	...	...	0.08	...	65.....	0.20	0.10	0.14	C
31.....	...	0.04	0.37	12.1	66.....	0.03	...	...	...
32.....	0.22	0.04	...	...	67.....	...	...	...	0.87
33.....	0.14	0.15	...	...	68.....	...	...	0.11	...
34.....	0.10	0.12	...	...	69.....	...	...	...	1.32
35.....	0.47	1.97	8.62	82.5	70.....	0.06	...	...	...

NOTE.—No entry indicates no detection; C indicates a confused source.

<sup>a</sup>Confused region composed of three known sources.

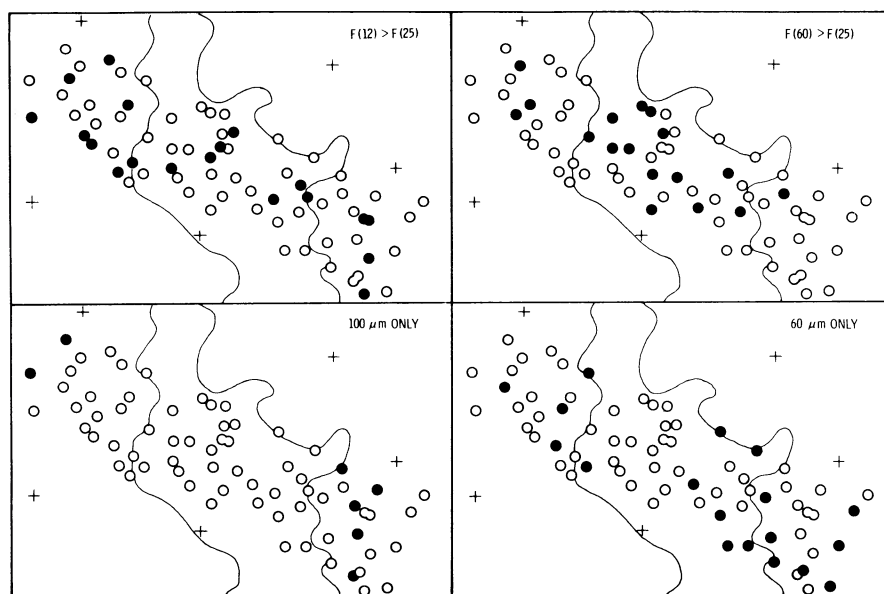


FIG. 2.—Distribution of the four subsamples discussed in the text

very few members of this subsample are galaxies. The identification of seven warm sources with previously known emission-line stars, HH objects, or embedded  $2\ \mu\text{m}$  sources suggests that many may be in the PMS stage. We conclude that the majority of these warm sources are probably recently formed stars associated with the cloud.

Many objects are found only at 60 or 100  $\mu\text{m}$ . Typically, signal-to-noise ratios exceed 10 but are usually lower than those of the warm sources. Three properties suggest that they are not an extension of the warm sample to lower luminosity, but they are a separate class of cooler ( $T_c < 60\ \text{K}$ ) objects. (1) Contrary to the warm objects, none of the cooler objects are near the cloud center, and a significant fraction (22 out of 25) lie outside or on the cloud boundary. This cannot be accounted for by confusion alone. (2) None are identified with the known HH objects or emission-line stars. (3) Many sources on the western side of the cloud appear to be correlated with small regions of enhanced extinction. Further work is required to confirm this correlation, but it suggests that many 60  $\mu\text{m}$  and 100  $\mu\text{m}$  only sources are associated with small globules surrounding the main cloud. These sources may be similar to the globules first found in the far-infrared by Keene *et al.* (1980) and may be the building blocks of the main cloud.

#### b) Infrared Luminosity of the Embedded 2 Micron Sources

Of the 29  $2\ \mu\text{m}$  objects found by HJM in the region of overlap with the present deep-sky field, only 7 were found to be associated with known PMS objects while the other 22 objects were unrelated field stars. None of the latter were detected in the present observations, but all PMS stars were found (sources 41, 42, 43, 44, 45; three were confused and appear as the source 41). The majority belong to the category of warm objects. Three additional objects were discovered in the region of overlap: 46 is a previously known emission-line star (Henize and Mendoza 1973); 48 is seen only at 12  $\mu\text{m}$ , and it is probably a field star. Source 47 is unidentified. Its warm spectrum suggests that it may also be a cloud member.

Integrating the energy distributions of the known PMS objects, we find a luminosity for  $\lambda \geq 12\ \mu\text{m}$  ranging from

0.04–0.18  $L_\odot$ . HJM find  $K$ -magnitudes similar to the PMS stars in Taurus (Cohen and Kuhi 1979) and near-infrared spectra consistent with spectral types between G8 IV and K8 IV. Cohen and Kuhi deduce for these spectral types in Taurus a total luminosity of 1  $L_\odot$ . Hence we conclude that the PMS objects discovered by HJM in Cha I emit not more than 5%–20% of their total luminosity at wavelengths longward of 12  $\mu\text{m}$ .

#### c) Low-Mass Star Formation Activity in Chamaeleon

The large fraction of warm sources that are identified with known PMS objects suggests that they will prove to be excellent tracers for low-mass star formation activity. About half of the warm sources (7 out of 13) within the cloud boundary have no known optical or  $2\ \mu\text{m}$  counterpart and may be more deeply embedded or lie on the far side of the cloud. Some of these may also be in an earlier evolutionary, collapsing stage, before the PMS phase. From their model calculations of the evolution of low-mass ( $1\ M_\odot$ ) protostars, Stahler, Shu, and Taam (1980) find that the earliest accretion phase lasts about  $10^5$  years. With an estimated PMS lifetime of a few  $10^6$  years, only a couple of objects in the Cha I cloud are likely to be in the gravitational collapse phase. Stahler, Shu, and Taam (1981) suggest that such objects are surrounded by a dense, optically thick photosphere of 200–400 K which would place them in the warm category. Unlike PMS sources, however, most of the total luminosity will be emitted at 10  $\mu\text{m}$  and longer. Hence, with *IRAS* data alone, one cannot easily distinguish low-luminosity embedded objects in the gravitational collapse phase from PMS objects that lie inside or on the far side of the cloud. Neither would show an optical counterpart, and both would have a relatively broad spectrum with comparable far-infrared luminosities. The important distinction between PMS objects and objects at the earliest stages of gravitational collapse will be the ratio of far-infrared to near-infrared luminosity.

We thank F. Shu for useful discussions.

#### REFERENCES

- Cohen, M., and Kuhi, L. V. 1979, *Ap. J. Suppl.*, **41**, 743.  
 Henize, K. G., and Mendoza, V. E. E. 1973, *Ap. J.*, **180**, 115.  
 Hyland, A. R., Jones, T. J., and Mitchell, R. M. 1982, *M.N.R.A.S.*, **201**, 1095 (HJM).  
 Keene, J. D., Harper, D. A., Hildebrand, R. H., and Whitcomb, S. E. 1980, *Ap. J. (Letters)*, **240**, L43.  
 Neugebauer, G., *et al.* 1984, *Ap. J. (Letters)*, **278**, L1 (Paper I).  
 Schwartz, R. D. 1977, *Ap. J. Suppl.*, **35**, 161.  
 Stahler, S. W., Shu, F. H., and Taam, R. E. 1980, *Ap. J.*, **241**, 637.  
 ———. 1981, *Ap. J.*, **248**, 727.  
 Soifer, B. T., *et al.* 1984, *Ap. J. (Letters)*, **278**, L71.